

# Modeling and Simulation of the Active Jammer Effect in the Crossed Array Detectors Infrared Seeker

S. Y. Alchekh Yasin  
Department of Electrical Eng  
IUST University  
Islamic Republic of Iran

A. R. Yrfanean  
Department of Electrical Eng  
Maleke-Ashtar University Islamic  
Republic of Iran

M. R. Mosavi  
Department of Electrical Eng  
IUST University  
Islamic Republic of Iran

A. Mohammadi  
Department of  
Aerospace Eng Maleke-  
Ashtar University Islamic Republic of  
Iran

## ABSTRACT

IR active jammers or the directed infrared counter measures (DIRCM) generate IR signals which attack the guidance signals passed to the sensors in IR-guided weapons. They provide IR signals with appropriate frequency, phase and intensity which will be superposed on those produced by the IR energy of the target passing through the reticle. When both the jamming signal and the modulated target energy signals are received by the missile's IR sensor, they cause the tracker to produce incorrect guidance commands and push the target out of the field of view (FOV). In this paper, the seeker signals of a crossed four slits or crossed array detectors (CAT) infrared seeker will be simulated. Then the active jammer signal is modeled and simulated. After that, the effect of all the active jammer parameters will be discussed and simulated. Finally, the conditions or the ranges of these parameters in which the active jammer can affect the seeking process will be stated.

## Keywords:

Infrared Seeker, Active Jammer, Crossed Array Detectors (CAT), Field of view (FOV).

## 1. INTRODUCTION

The countermeasures are required in modern war in order to protect the targets from the advanced missiles that could be a threat and damage to those. Therefore, the homing missile requires a Counter Counter-Measure (CCM) to remove or overcome the effects of countermeasures for efficient target tracking [1-6]. In general, the IR missiles utilize the thermal energy radiated or reflected by the target. Usually they have a single IR detector and reticle to detect target. The reticle used in an infrared seeker separates an IR target from its background and produces appropriate modulation signals that make possible a variety of signal processes for target tracking [7-9].

To provide powerful Infrared CCM (IRCCM) techniques a seeker of two-color IR channels is used [10]. This seeker uses single reticle with two detection bands (M band) in mid IR

region and (N band) in near IR region. Therefore up to the spectral distribution difference of target and flares due to their temperature difference the seeker can distinguish between them.

The structure of the crossed ship reticle or the crossed four slits reticle (Actually it is equivalent to a reticle with four crossed array detectors), which is a stationary reticle type, will be stated with the design parameters. This type employs a fixed reticle, with radius  $R_a$  and  $N=4$  transparent sectors or slits, and a slightly tilted rotating mirror or lens (with spinning frequency  $f_m$ ) to sweep the Target Image Spot (TIS) along a circular path on the reticle Target Imaging Circle (TIC) with constant radius ( $R_N$ ), as shown in Fig. 1. The distance of the non-concentric TIC centre and its phase relatively to the reticle centre define the position of the target in the FOV [7-9]. In Fig 1,2 the defined parameters:

- $D$ : the spoke width or the detector width (pixel).
- $L$ : the spoke length or the detector length (pixel).
- $R_a$ : the reticle radius (FOV radius) (pixel).
- $R_N$ : the target imaging circle (TIC) (pixel).

In this study, these parameters take the following values: ( $D=70$ ,  $L=850$ ,  $R_N=615$ ,  $R_a=885$ ) unit or pixel.

When the TIC is not concentrate with the reticle, which means that the target position is not on the center of the FOV, we can define the imaging circle center (or the target position) parameters ( $\alpha_T(t)$ ,  $\beta_0(t)$ ), as shown in Fig. 3. In addition to that, important parameters, which specify the TIS position in a certain instant  $t$ , can be defined:

- $\varphi(t)$ : the TIS phase in the instant  $t$  in a reference system related to the TIC.
- $\beta(t)$ : the TIS phase in the instant  $t$  in a reference system related to the reticle.
- $r_0(t)$ : the TIS radius in the instant  $t$ .
- $x_T, y_T$ : the TIC center coordination in a reference system related to the reticle.

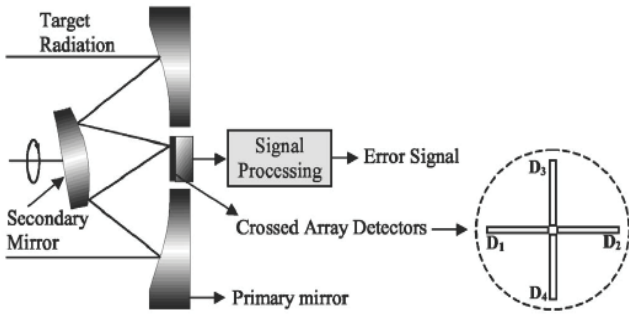


Fig. 1: The crossed array detectors infrared seeker.

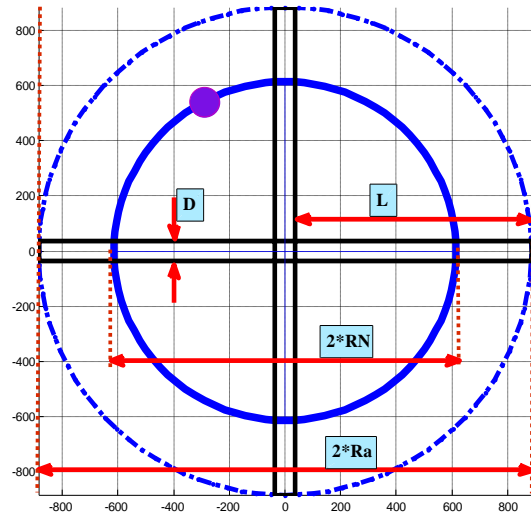


Fig. 2: The design parameters of a CAT reticle (D,L, Ra, RN).

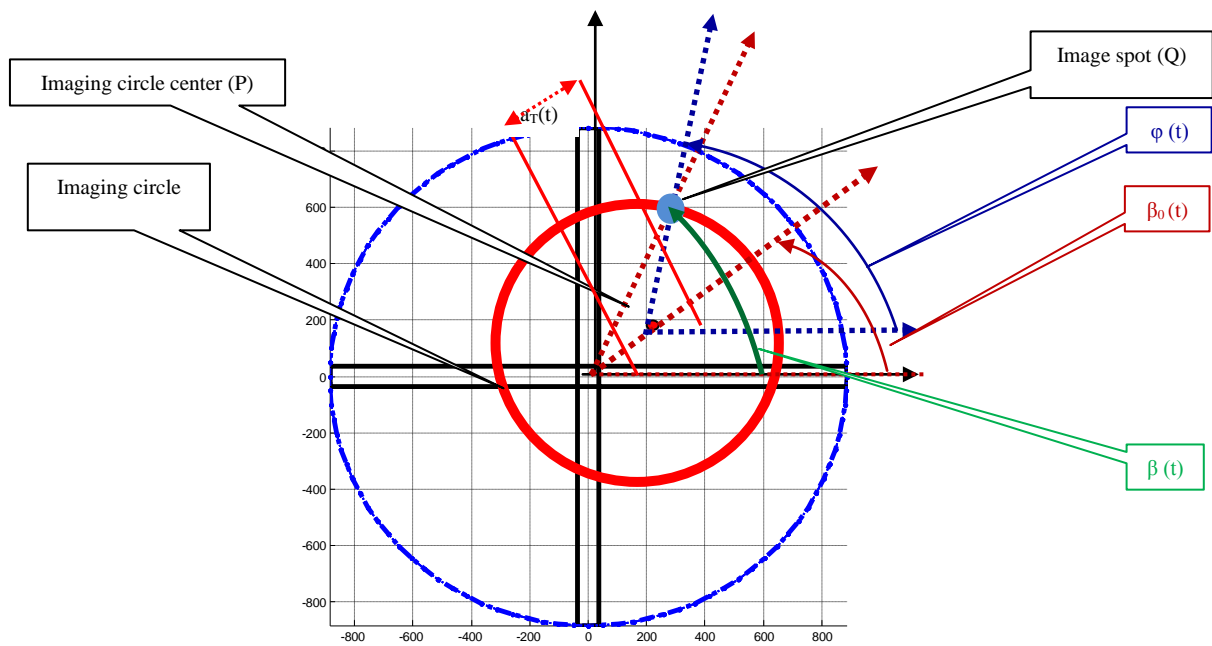


Fig. 3: The analyze parameters (  $\beta_0(t)$ ,  $\beta(t)$ ,  $\phi(t)$ ,  $r_0(t)$ ,  $a_R(t)$  ).

The proposed reticle model takes the reticle parameters (D, L, Ra, RN) as inputs and gives the output signal up to the target position parameters, such as the coordination in the Field Of View (FOV).

To modulate the two-color seeker, a model of a detector with variant band limits,  $[\lambda_{min1}, \lambda_{max1}]$  for the (M band) in mid IR region and  $[\lambda_{min2}, \lambda_{max2}]$  for the (N band) in near IR region. The detectors outputs ( $D_{1T}, D_{2T}, D_{1J}, D_{2J}$ ) will form the two color channels by combining with the reticle outputs [10-13].

All the modeling and simulation tasks and processes will be designed and developed using the MATLAB® tools and packages.

## 2. SEEKER MODELING RELATIONS

Every object over 0K emits IR radiation depending on its temperature and its spectral distribution is given as a function of temperature by Planck's law as follows :

$$W(T, \lambda) = \frac{2 \cdot \pi \cdot h \cdot c^2}{\lambda^5 \cdot (e^{\frac{h \cdot c}{\lambda \cdot T}} - 1)} = \frac{c_1}{\lambda^5 \cdot (e^{\frac{c_2}{\lambda \cdot T}} - 1)} \quad (1)$$

where  $c_1$  and  $c_2$  are the first and second radiation constants, and  $k$ ,  $h$ ,  $\lambda$ , and  $T$  are the Boltzman's constant, the Planck's constant, the wavelength, and absolute temperature. The IR normalized spectral distributions depend strongly on temperature; the spectrum peak moves to shorter wavelength as the temperature rises, as shown in figure 4.

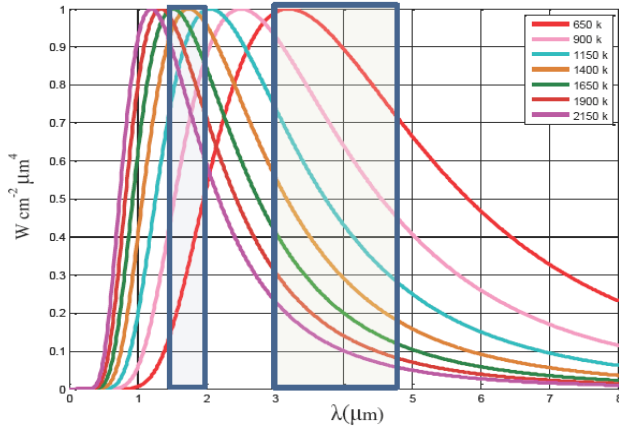


**Fig.4. Normalized spectral distributions of IR sources. The shaded spectral regions represent the N and M bands.**

The output of the detector on the M band which is defined by  $[\lambda_{min1}, \lambda_{max1}]$  is given by:

$$D_1(t) = D_{[\lambda_{min1}, \lambda_{max1}]}(T(t)) = \int_{\lambda_{min1}}^{\lambda_{max1}} W(T(t), \lambda) . d\lambda(2)$$

Similarly, the output of the detector on the N band which is defined by  $[\lambda_{min2}, \lambda_{max2}]$  is given by:

$$D_2(t) = D_{[\lambda_{min2}, \lambda_{max2}]}(T(t)) = \int_{\lambda_{min2}}^{\lambda_{max2}} W(T(t), \lambda) . d\lambda(3)$$

As a result, the outputs of two-color detectors in the existence of a target and a jammer are:

$$D_{1T}(T(t)) = D_1(T_T(t)), D_{2T}(T(t)) = D_2(T_T(t))(4)$$

$$D_{1J}(T(t)) = D_1(T_J(t)), D_{2J}(T(t)) = D_2(T_J(t))(5)$$

Or

$$D_{1T}(T[n]) = D_1(T_T[n]), D_{2T}(T[n]) = D_2(T_T[n])(6)$$

$$D_{1J}(T[n]) = D_1(T_J[n]), D_{2J}(T[n]) = D_2(T_J[n])(7)$$

On each detector all IR radiations pass through the reticle and become modulated signals; therefore, these modulated signals will be integrated on the surface of the detector with weights related to the temperature and surface of each target or flare. So the channels signals can be written as:

$$Y(ch1) = Rad(T_T, S_T) * m_T[n] + Rad(T_J, S_J) * m_J[n] (8)$$

$$Y(ch1) = H_1(S_T) * D_{1T}[n] * m_T[n] + H_1(S_J) * D_{1J}[n] * m_J[n] (9)$$

$$Y(ch2) = H_2(S_T) * D_{2T}[n] * m_T[n] + H_2(S_J) * D_{2J}[n] * m_J[n] (10)$$

Where  $m_J, m_T$  are the modulations resulting from the reticle on the target and the jammer signals respectively.

Actually, H1 and H2 can be generalized to include all the external parameters distributed from the target or the flare to the detectors. Therefore, by taking into accounts that (H1=H2) is the same for the same IR object and by normalizing relatively to the target, the relations can be rewrite:

$$Y(ch1) = Y_{1T}[n] + Y_{1J}[n], Y(ch2) = Y_{2T}[n] + Y_{2J}[n](11)$$

Where

$$Y_{1T}[n] = \gamma_T * D_{1T}[n] * m_T[n]$$

$$Y_{2T}[n] = \gamma_T * D_{2T}[n] * m_T[n](12)$$

$$Y_{1J}[n] = \gamma_J * D_{1J}[n] * m_J[n]$$

$$Y_{2J}[n] = \gamma_J * D_{2J}[n] * m_J[n] (13)$$

### 3. ACTIVE JAMMER MODELING

For an active jammer it has to define:

$$M(x, y) = \Delta(n_1, N_1) + \Delta(n_2, N_2) + \Delta(n_3, N_3) + \Delta(n_4, N_4)(14)$$

$$n_i = P_i(x, y), N_i = W_i(x, y) \dots \dots i = 1, 2, 3, 4(15)$$

$$m_T(x_T, y_T, r_T) = M(x_T, y_T) * \Phi(x_T, y_T, r_T)(16)$$

$$\Phi(x_T, y_T, r_T \cong 0) = 1(17)$$

$$m_J(x_J, y_J) = m_J(x_T, r_T) = M(x_T, y_T) * \varphi(t)(18)$$

$$\varphi(t) = [0.5 + 0.5 * \cos(2 * \pi * f_J * t + \theta_J(t))](19)$$

So:

$$m_J(x_J, y_J) = m_J(x_T, r_T) = M(x_T, y_T) * [0.5 + 0.5 * \cos(2 * \pi * f_J * t + \theta_J(t))](20)$$

Where  $f_J, \theta_J$  are the jammer signal frequency and phase respectively. And as a result the seeker signals will be:

$$Y(ch1) = \gamma_T * D_{1T}[n] * M(x_T, y_T) * \Phi(x_T, y_T, r_T) + \gamma_J * D_{1J}[n] * M(x_T, y_T) * \varphi(t)(21)$$

$$Y(ch1) = M(x_T, y_T) * \{\gamma_T * D_{1T}[n] * \Phi(x_T, y_T, r_T) + \gamma_J * D_{1J}[n] * \varphi(t)\}(22)$$

$$Y(ch1) = M(x_T, y_T) * A * \{\Phi(x_T, y_T, r_T) + \eta * [0.5 + 0.5 * \cos(2 * \pi * f_J * t + \theta_J(t))]\}(23)$$

With:

$$\max \|M(x_T, y_T)\| = \max \|\Phi(x_T, y_T, r_T)\| = \max \|\varphi(t)\| = 1, \eta[n] = \frac{\|Y_{1J}[n]\|}{\|Y_{1T}[n]\|} > 1(24)$$

For a certain target and a certain active jammer:

$$\eta = Const(S_T, S_J) * Const(T_T, T_J) = \frac{\gamma_J}{\gamma_T} \cdot \frac{D_{1J}}{D_{1T}} = \eta_1 * \eta_2(25)$$

Figure 5 shows the following case:

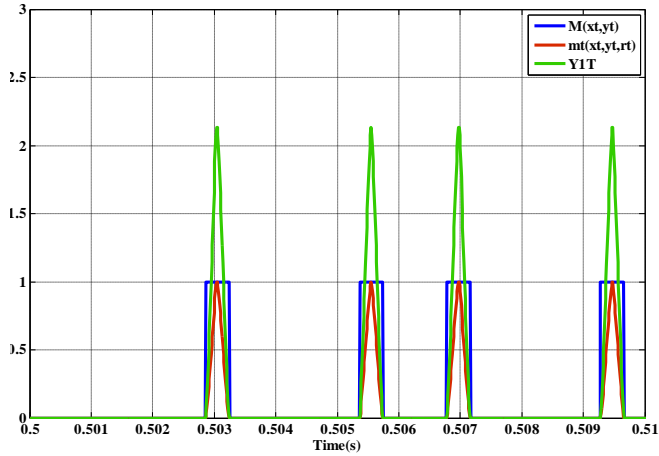
#### ❖ Target

- temperature: 850k. so  $D_{1T} = 1.07, \gamma_T = 2$ .
- $dx = dy = 1000 \text{ pixel/s}$ .

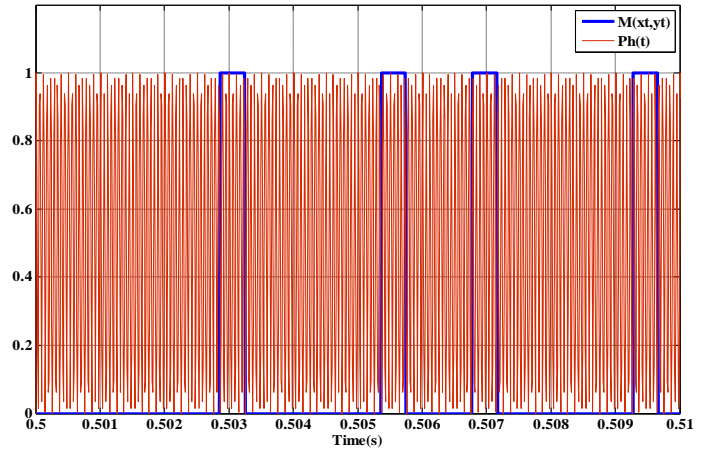
#### ❖ Jammer

- temperature: 1500k. so  $D_{1T} = 7.9, \gamma_J = 0.3$ .
- $f_J = 18000 \text{ Hz}$ , Phase=0 degree.

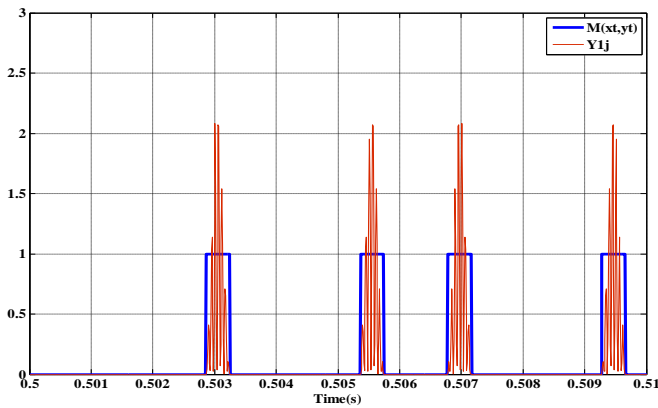
$$\text{❖ So : } \eta = \frac{\gamma_J}{\gamma_T} \cdot \frac{D_{1J}}{D_{1T}} = \eta_1(0.15) * \eta_2(7.36) = 1.1$$



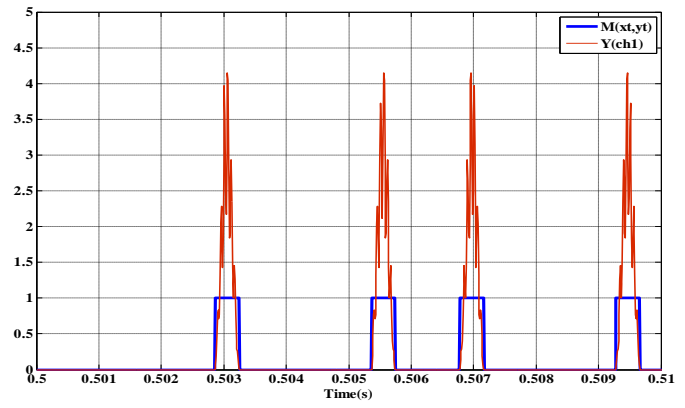
(a)  $M(x_T, y_T)$ ,  $m_T(x_T, y_T, r_T)$ ,  $Y_{1T}$



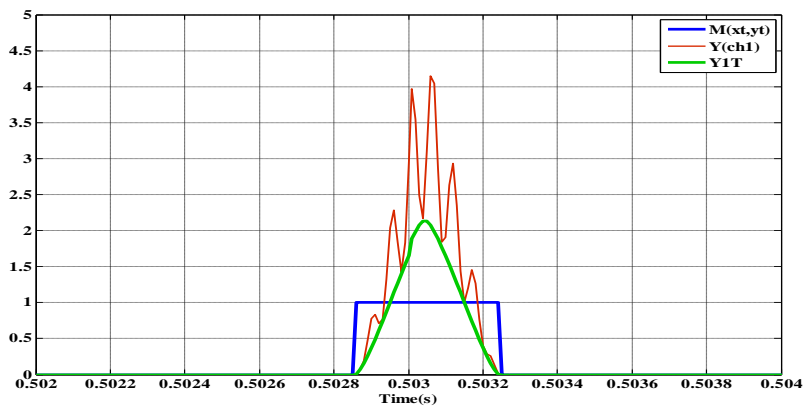
(b)  $M(x_T, y_T)$ ,  $\phi(t)$



(c)  $M(x_T, y_T)$ ,  $Y_{1J}$



(d)  $M(x_T, y_T)$ ,  $Y(ch1)$



(e)  $M(x_T, y_T)$ ,  $Y(ch1)$

Fig.5: Seeker signals in the case of a target (temperature: 850k. so  $D_{1T} = 1.07$ ,  $\gamma_T = 2$ ,  $dx = dy = 1000$  pixel/s) and a jammer (temperature: 1500k. so  $D_{1J} = 7.36$ ,  $\gamma_J = 0.3$ ,  $f_j = 18000$ Hz).

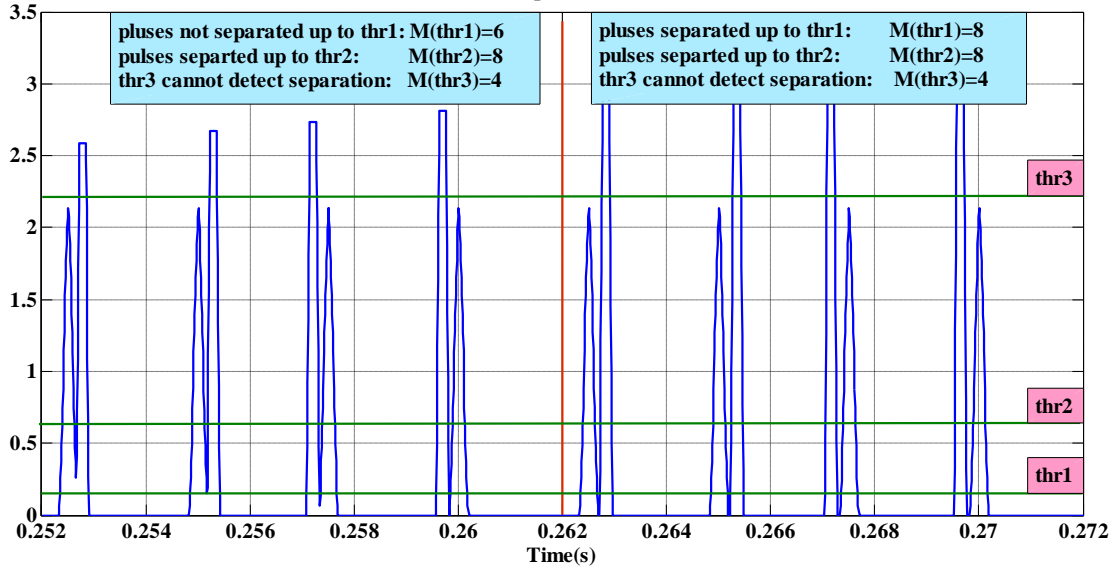


Fig.6: Pulses determination up to a constant threshold (th1=0.1).

#### 4. ACTIVE JAMMER EFFECT

The effect of the jammer depends on the process of dialing with the case of number of pulses more than 4. Clearly the jammer will be effect when it can produce pulses more than 4 as shown in Fig 6. For studying the influence of the jammer the seeking will be stopped when the pulse number more than 4 up to the constant threshold. The effect of the jammer parameters will be studied by its parameters: the jammer frequency, phase and amplitude.

##### 4.1.The Jammer Frequency and Phase Effect

From the figure 2, the minimum pulse width can be calculated:

$$w_{min} = T_m \cdot \left( \frac{D}{2\pi \cdot R_N} \right) = 0.01 * \left( \frac{70}{2\pi \cdot 615} \right) = 1.8115 \cdot 10^{-4} s(26)$$

Or

$$w_{min} = \frac{T_m}{T_s} \cdot \left( \frac{D}{2\pi \cdot R_N} \right) = \frac{0.01}{0.0001} * \left( \frac{70}{2\pi \cdot 615} \right) = 18 Ts \quad (30)$$

Where  $T_s$  is the sampling period, and  $T_m$  is the spinning period.

Clearly, for a small spot radius ( $r_T=1$  pixel), if the jammer signal period is bigger than twice  $w_{min}$  this signal will not be able to affect the seeking whatever its amplitude and phase:

$$2w_{min} < T_j \rightarrow f_j < f_{j1} = 0.5 * f_{jmin} = 2.75kHz(31)$$

Also, if the jammer signal period is less than this value  $w_{min}$  the signal affects the seeking whatever the phase but it is related to the amplitude value:

$$w_{min} > T_j \rightarrow f_j > f_{j2} = f_{jmin} = 5.5kHz(32)$$

On the other hand, if the jammer frequency in the range  $F(r_T=1pixel) = [f_{j1}, f_{j2}]$ , which depends on the spot radius  $r_T$ , the influence depends on the amplitude and the phase of the signal.

Any way the effect in this range is limited as it depends on the phase. So the main range for the influence is defined by:

$$f_j > f_{j0} = f_{jmin}(r_Tmin = 1pixel) = 5.5kHz(33)$$

For a frequency  $f_j > f_{j0}$  each pulse will divide into multiple pulses or a group of pulses, and these pulses distribute around the main pulse position and within an interval equals to the main pulse width as shown in Fig 5 (e). The number of the pulses in this group is related to the jammer frequency, and it can be calculated approximately by the relation:

$$flour\left(2 * \frac{w}{T_j}\right) = round\left(2 * \left(\frac{f_j}{f_{j0}}\right)\right) \leq n \leq round\left(2 * \frac{w}{T_j}\right) = round\left(2 * \left(\frac{f_j}{f_{j0}}\right)\right)(34)$$

So the pulse number in a spin period is :

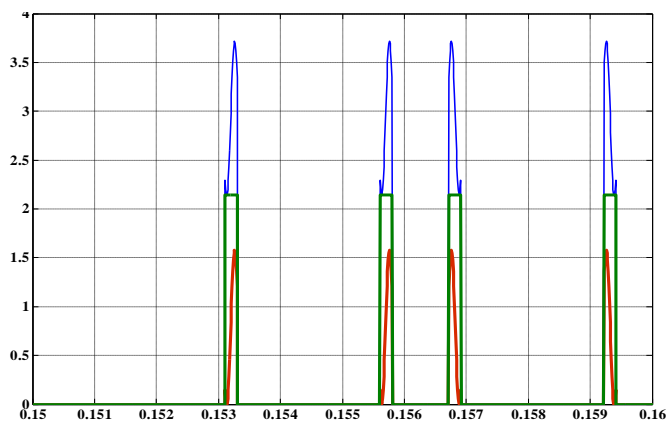
$$4 * flour\left(2 * \left(\frac{f_j}{f_{j0}}\right)\right) \leq N = 4 * n \leq 4 * round\left(2 * \left(\frac{f_j}{f_{j0}}\right)\right)(35)$$

- For  $f_j \in [0.5 * f_{j0}, f_{j0}]$ :  $4 \leq N \leq 8$  up to the phase .
- For  $f_j = f_{j0}$ :  $N = 4 * n = 8$  for any phase.
- For  $f_j = 1.5 * f_{j0}$ :  $8 \leq N \leq 12$  up to the phase.

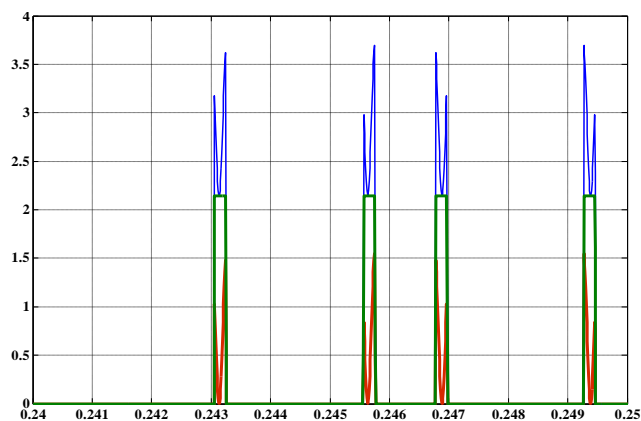
The results can be summarized in the table 1, and can be shown in Fig 7,8.

Table 1: The jammer frequency effect

$f_j < 0.5 * f_{j0}$	$0.5 * f_{j0} \leq f_j < f_{j0}$	$f_{j0} \leq f_j$
No effect whatever the amplitude and the phase.	The effect is related to the amplitude and the phase.	The effect is related to the amplitude.

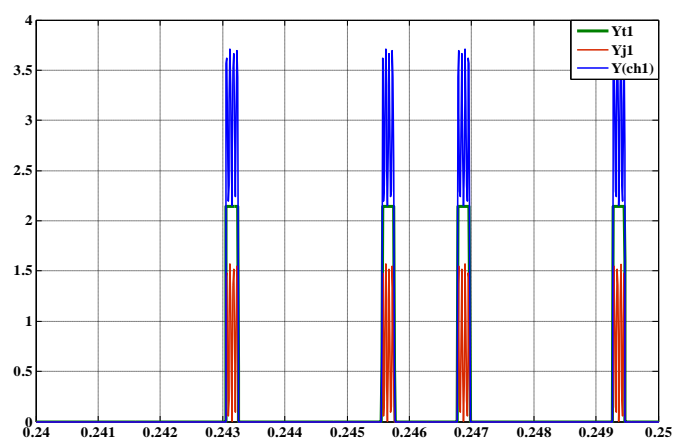


(a) The phase allow the jammer to produce new pulses.

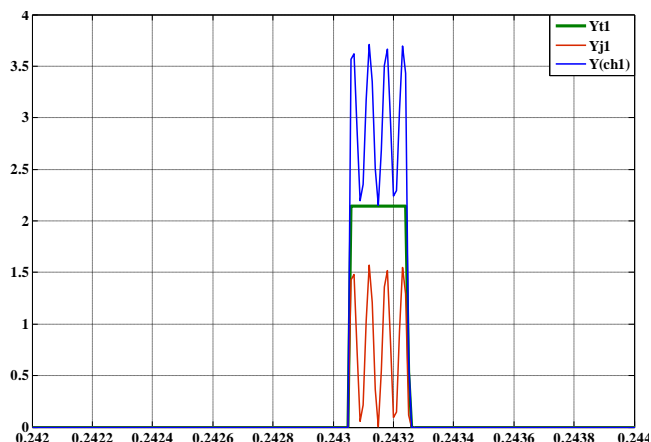


(b) The phase does not allow the jammer to produce new pulses.

**Fig. 7 :** The seeker signals for a target (temperature: 850k,  $D_{1T} = 1.07$ ,  $\gamma_T = 2$ ,  $dx = dy = 1000$  pixel/s) and a jammer (temperature: 1500k,  $D_{1J} = 7.36$ ,  $\gamma_J = 0.3$ ,  $f_j=4$ kHz). In this case  $0.5 * f_{j0} \leq f_j < f_{j0}$  so the jammer can produce new pulses but it is related to the phase difference, and this phase difference cannot be controlled as it is related to the target position on the reticle or in the FOV.



(a)



(b)

**Fig. 8** The seeker signals for a target (temperature: 850k,  $D_{1T} = 1.07$ ,  $\gamma_T = 2$ ,  $dx = dy = 1000$  pixel/s) and a jammer (temperature: 1500k,  $D_{1J} = 7.36$ ,  $\gamma_J = 0.3$ ,  $f_j=18$ kHz). In this case  $f_{j0} \leq f_j$  so the jammer can produce new pulses whatever the phase of the signal, in this case the pulse number is  $N=4 * 4 = 16$

## 4.2. The Jammer Amplitude Effect

The effect of the jammer signal amplitude is measured by the effect of the parameter:

$$\eta[n] = \frac{\|Y_{1J}[n]\|}{\|Y_{1T}[n]\|}$$

which measures the effect of the jammer up to its relative amplitude. Several values of the threshold (thr1), which is the reference level up to which the pulses number is determined, will be considered, then the minimum relative amplitude  $\eta_{\min}$  (thr1) will be determined. For a **thr1=0.75**, the jammer amplitude is changed until the seeker miss the real target as shown in Fig 9, in this case the minimum relative amplitude is gotten. Clearly from the previous example that each pulse detection threshold value (thr1) requires a minimum relative

amplitude of the jammer which has to be able to make the threshold detecting the existence of the multiple pulses resulting from the jammer influence. Also, it is clear that the smaller threshold requires bigger relative jammer amplitude, and vice versa. The table 2 shows the required minimum relative amplitude ( $\eta_{\min}$ ) for several values of the pulse detection threshold.

**Table 2 :  $\eta_{\min}$  (thr1)**

thr1	1.6	0.7	0.35	0.2	0.1
$\eta_{\min}$	1.8	3.6	7.2	14.4	29

This result can be explained as following. Suppose the target signal before the jammer switching on:

$$Yt1 < Thremx1(36)$$

Where Thremx1 is the AGC threshold. After the switching on, the AGC will make multiple steps (n) to prevent the saturation, the jammer will effect if the target signal after this AGC step become less than the pulse detection threshold. So for the minimum relative amplitude:

$$\eta > \eta_{min} \rightarrow Yt1 * (Atenu1)^n < thre1 \text{ jammer can effect}$$

$$\eta < \eta_{min} \rightarrow Yt1 * (Atenu1)^n > thre1 \text{ cannot effect}$$

$$\eta = \eta_{min} \rightarrow Yt1 * (Atenu1)^n \approx thre1(37)$$

Where Atenu1 is the AGC attenuation step. So :

$$\begin{aligned} Thremx1 * Atenu1 < Y(ch1) * (Atenu1)^n \\ = (Yt1 + Yj1) * (Atenu1)^n < Thremx1 \end{aligned}$$

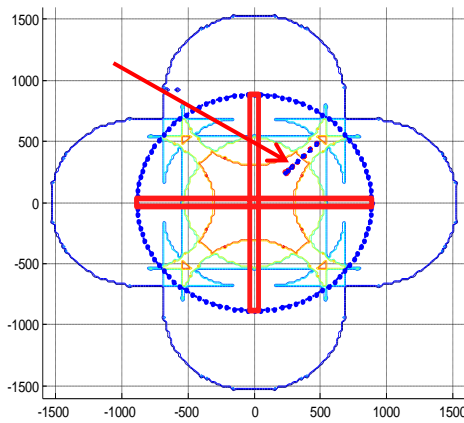
$$\frac{Thremx1}{thre1} * Atenu1 < \frac{Yt1 + Yj1}{Yt1} < \frac{Thremx1}{thre1}$$

$$\eta_{min} \in \left[ \frac{Thremx1}{thre1} * Atenu1 - 1, \frac{Thremx1}{thre1} - 1 \right] (38)$$

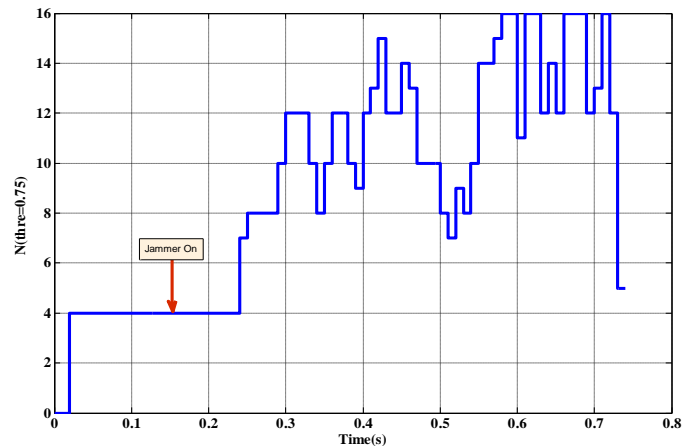
The table 3 shows a comparison between the simulation results and the relation (38). Clearly, the threshold cannot be so big (> 1V) to avoid miss the detection of real target in the case of weak signal. On the other hand, the threshold cannot be so small (< 0.1 V) to avoid the influence of the noise. For small threshold in this cas the relative amplitude is big and may cannot be provided.

Table 3: Thremax=3.5, Atenu1=0.75

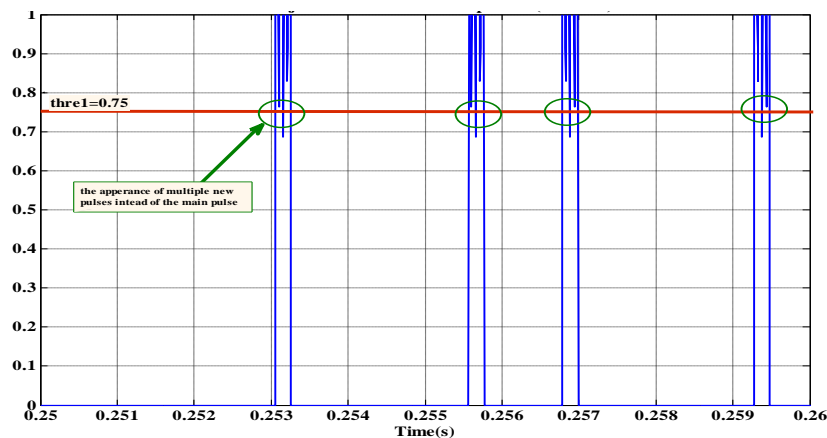
thre1	1	0.7	0.35	0.2	0.1
$\eta_{min}$	1.8	3.6	7.2	14.4	29
$\eta_{min}(\text{relation})$	[1.6, 2.5]	[2.75, 4]	[6.5, 9]	[12, 16]	[25, 34]



(a) The FOV shows missing the target after the jammer is switched on.



(b) The pulses number relative to the constant threshold (thre1=0.75), an increasing in this number can be shown after the jammer is switched on.



(c) The multiple AGC steps push the signal down in a manner that the pulses can be detected by the threshold.

Fig. 9 The effect of a jammer (temperature: 1500k,  $D_{1J} = 7.36$ ,  $\gamma_J = 1$ ,  $f_j = 18\text{kHz}$ ,  $\eta = 3.67$ ) on the seeking of a target (temperature: 850k,  $D_{1T} = 1.07$ ,  $\gamma_T = 2$ ,  $dx = dy = 1000 \text{ pixel/s}$ ).

## 5. CONCLUSION

In this paper, it analyzes the jamming effect of the DIRCM jammer signal to oppose the crossed array detectors reticle seeker through the simulation. The simulation results show that the jamming effect is greatly influenced by frequency, phase and intensity of the jammer signal. Specially, the jammer frequency has the largest influence on the jamming effect. The jammer frequency has to be more than a certain value to be able to affect the seeking process. In addition to that, the jammer intensity has to be more than a certain value related to the pulse position technique to be able to produce effective influence on the seeker signals. As a result, the jammer has to be with appropriate parameters for influence the guidance signals in a manner that the target will be pushed out of the FOV and be missed, or causes an unstable situation in the seeking making the miss distance is so large.

## 6. REFERENCES

- [1] D. H. Titterton. "A review of the development of optical countermeasures". Proceedings of SPIE, 5615, December 2004.
- [2] J. Heikell. "Electronic warfare self-protection of battlefield helicopters: A holistic view". Helsinki University of Technology, Applied Electronics Laboratory Series E: Electronics Publications E18, Espoo-Finland, 2005.
- [3] J. D. Ovest, "Global Mobility : Anywhere, Anytime, any Threat? Countering the MANPADS Challenge", Air University Maxwell Air Force Base, Alabama, Occasional Paper No. 38, December 2005.
- [4] D. Maltese, J. Robineau, "Countering MANPADS : Study of New Concepts and Applications", Defense and Security Division, Proc. of SPIE Vol. 6203 62030G-2, 2006.
- [5] M. Puttre, "LIFE Closes the Loop," The Journal of Electronic Defense 24, no. 7 (July 2001), 25.
- [6] "Protecting the Big Boys: Directed IR Countermeasure for Large Aircraft," Journal of Electronic Defense 23, no. 12 (December 2000), 48.
- [7] Z. W. Chao and J. L. Chu, "General Analysis of Frequency-Modulation Reticles," Opt. Eng. 27, 440–442 (1988).
- [8] M. A. Porras, J. Alda, and E. Bernabeu, "Amplitude-Modulated and Frequency-Modulated Reticule Responses of Gaussian Beams," Optical Engineering, Vol. 30, No. 12 (1991).
- [9] R. G. Driggers, C. E. Halford, and G. D. Boreman, "Use of Spatial Light Modulators in Frequency Modulation Reticule Trackers," Optical Engineering. Vol. 29, No. 11, pp. 1398-1403 (1990).
- [10] W. Haifeng, L. Zhi, Z. Qing, and S. Xinzhi, "A Double Infrared Image Processing System Using Rosette Scanning," Proceeding. SPIE, Vol. 2894, pp. 2-10 (1996).
- [11] D. P. Forrai and J. J. Maier, "Generic Models in the Advanced IRCM Assessment Model," Proceeding of the 2001 Winter Simulation Conference, pp. 789-796 (2001).
- [12] M. R. Mosavi, M. Asadpour, and R. Kalili, "Comparing Performance of Two Infrared Anti-Jamming Methods using Fuzzy System and Neural Network," 2007 Congress on Intelligent and Fuzzy Systems, Ferdowsi University of Mashhad, Iran (2007).
- [13] M. R. Mosavi, M. Asadpour, and H. A. Amerim, "Design and Simulation of an Infrared Jammer Source for an Infrared Seeker," IEEE Conference on Signal Processing, Communications, and Networking, India (2008).